Electronic structure of $KNbO_3$ and $KTaO_3$

T. Neumann, G. Borstel, C. Scharfschwerdt, and M. Neumann
Fachbereich Physik, Universität Osnabrück, Barbarastrasse 7, D-4500 Osnabrück, Federal Republic of Germany
(Received 6 February 1992; revised manuscript received 29 June 1992)

The electronic structure of cubic $KNbO_3$ and $KTaO_3$ has been calculated using the self-consistent, scalar-relativistic linear-muffin-tin-orbital method. The calculated density of states (DOS) shows a strong similarity for both materials and is in good accordance with measured photoelectron spectra (PES). The projected DOS reveals a strong d-band character for the valence band, which is due to an evident hybridization of O $2p$ states with the unoccupied Nb(Ta) d states. This is also confirmed by PES data, if one makes use of the Cooper minimum for d bands. The calculation underestimates the band gaps by about 50%, a result that is known also from other band calculations for insulators within density-functional theory. Ground-state properties are obtained from total-energy calculations. Lattice constants agree within a few percent with experimental ones. The bulk modulus for $KTaO_3$ (2.25 Mbar) is in good agreement with experiment, while for $KNbO_3$ (2.47 Mbar) it is nearly twice as large as the experimental value. Cohesive energies are found to be -42.2 eV for $KNbO_3$ and -44.5 eV for $KTaO_3$ (per unit cell). Corresponding experimental values do not seem to exist in standard literature.

I. INTRODUCTION

Among the large number of perovskites with chemical formula ABO_3 the most extensively investigated compounds are $BaTiO_3$, $KNbO_3$, $KTaO_3$, and $SrTiO_3$. Interest in these systems has been stimulated to a large extent by their unusual dielectric properties[1] and by the observation of superconductivity in semiconducting samples of $SrTiO_3$.[2]

Because of its ferroelectric transition near room temperature, $BaTiO_3$ represents the most studied ferroelectric crystal, both theoretically and experimentally. First-principles theoretical studies of its electronic structure and the origin of ferroelectricity started in 1985 and were performed using the linearized-muffin-tin-orbital[3,4] (LMTO) and the linearized-augmented-plane-wave[5] method. For $SrTiO_3$ results of state-of-the-art advanced bandstructure calculations have been reported so far by only one group[3,4] using the LMTO method. $KNbO_3$ has recently been studied using the selfconsistent orthogonalized linear combination of atomic orbitals[6] (OLCAO) method, where orbitals from partially ionized atoms are used for the basis set. However, practically no modern first-principles calculations exist in the case of $KTaO_3$ crystals. Except for Ref. 6, electronic-structure calculations for $KNbO_3$ and $KTaO_3$ reported in literature are either not self-consistent,[7] use parametrized empirical models,[8,9] or are based on a cluster description of the solid.[10] On the other hand, the expectation that doped crystals of $KNbO_3$ might be new candidates for electrooptic devices has led recently to an increasing number of experimental investigations of these systems.[11] It was essentially these facts that motivated us to start the present study on $KNbO_3$ and $KTaO_3$.

The organization of this paper is as follows: In Sec. II we give a comprehensive description of calculational aspects when applying the LMTO method to perovskites. The results of the present calculation are presented in Sec. III. In Sec. III A we discuss ground-state properties; band structures are shown in III B and compared to photoelectron spectra in III C. In Sec. III D a discussion of the calculated charge distribution is given.

II. DETAILS OF CALCULATION

The electronic-structure calculations for the perovskites have been performed using the LMTO method of Andersen.[12] We used the scalar-relativistic form of this method, i.e., including the relativistic band shifts but neglecting the spin-orbit splitting. The exchange-correlation potential of density-functional theory[13,14] (DFT) has been obtained in the local-density approximation (LDA) of von Barth and Hedin.[15] As the method is described in detail elsewhere,[12,16] we will give only a brief account of the most important computational details.

$KNbO_3$ and $KTaO_3$ were calculated in the ideal cubic perovskite structure. We thus neglect the slight noncubic distortions in the crystal structure of $KNbO_3$ below 418 °C.[1] $KTaO_3$ is known to remain cubic down to at least 1.6 K.[1]

Within the atomic sphere approximation[12] (ASA) of the LMTO method, which has been applied in the present calculations, the crystal potential is constructed of overlapping Wigner-Seitz spheres for each atom in the unit cell. The ratio between the sphere radii has been chosen in accordance with a more recent LMTO-ASA calculation for cubic $NaWO_3$,[17] to be $S_A{:}S_B{:}S_O = 2{:}1.5{:}1$. With lattice constants $a(KNbO_3) = 7.44$ a.u., and $a(KTaO_3) = 7.40$ a.u., which were calculated from the condition of minimal total energy in the ground state (see Sec. III A), this means for $KNbO_3$ $S_K = 3.80$ a.u., $S_{Nb} = 2.85$ a.u.,

TABLE I. Valence states and atomic occupation number Σ.

Atom	Valence states	Σ
K	$4s^1\,3p^6\,/4p^0\,3d^0$	7
Ta	$6s^2\,6p^0\,5d^3$	5
Nb	$5s^1\,5p^0\,4d^4$	5
O	$2s^2\,2p^4\,3d^0$	6

and $S_O = 1.90$ a.u., and for $KTaO_3$ $S_K = 3.79$ a.u., $S_{Ta} = 2.84$ a.u., $S_O = 1.89$ a.u., respectively. Thus with the latter ratio of S_A, S_B, S_O the sphere radii of the metal atoms fall close to the atomic radii $S_K = 4.29$ a.u. and $S_{Nb} = S_{Ta} = 2.76$ a.u. of the corresponding pure metal phases.[18]

According to the spirit of the LMTO procedure, only the energetically higher-lying valence states have been included in the self-consistent calculation of the effective crystal potential; see Table I. The deeper-lying core states are treated as atomiclike in the so-called frozen-core approximation.[16] For the valence states the maximum angular momentum $l_{\max}$ for the l summation of the muffin-tin orbitals has been taken to be $l_{\max} = 2$ for all types of atoms.

In order to minimize the error due to the energy linearization in the basis functions, we have split the total energy range into two panels, one for the $O(2s)/K(3p)$ states and one for the valence and unoccupied bands. The calculations were iterated to self-consistency with an error in total energies less than 0.1 mRy.

III. RESULTS

A. Ground-state properties

In this section we present our results for true ground-state properties of the systems, derived from the corresponding total energy E_0. More accurately, we will refer only to the valence part E_0^{val} of the total energy, which is E_0 minus the constant contribution of the core states, which was treated in the frozen-core approximation (cf. Sec. II). The results are shown in Table II.

The lattice constant has been obtained by locating the minium of E_0^{val} as a function of a (a_{energy}) and alternatively by determing that value of a where the electronic pressure of the system vanishes (a_{pressure}). The pressure at $T = 0$ K was calculated, using the virial theorem, where it is given as a summation of surface integrals over the atomic spheres plus the Madelung energy.[19] Theoretical and experimental lattice constants in Table II agree within a few percent relative error. The agreement is slightly better for a_{pressure}.

From the variation of the pressure with the lattice constant, we can also derive the theoretical bulk modulus $B = -V\,(dP/dV)$. Comparing these values with bulk moduli, calculated from corresponding experimental elastic constants, one finds an agreement within a few percent in the case of $KTaO_3$, whereas the difference for $KNbO_3$ is in the range of 50%. This strong deviation may be due to a relatively high uncertainty of about 20% (according to the author of Ref. 21) in the experimentally derived elastic constants. Another reason may be that the theoretical B has been calculated in the cubic phase at 0 K, while the $KNbO_3$ crystal is known to be cubic only in the high-temperature phase.

The calculated cohesive energy E_{coh} for $KTaO_3$ is slightly larger than that for $KNbO_3$. This trend does not correspond to experimental cohesive energies derived from a Born-Haber cycle, where E_{coh} for $KTaO_3$ is about 17% smaller than E_{coh} for $KNbO_3$. Comparing absolute values, one finds the measured cohesive energy 17% ($KNbO_3$) and 35% ($KTaO_3$) smaller than the corresponding calculated LMTO-ASA value. It should, however, be mentioned, that the quality of the experimental data depends on the heat of reaction of $Nb_2O_5(c) + K_2O(c) \rightarrow 2\ KNbO_3(c)$ [-13.82 eV (Ref. 23)] and $K(c)+Ta(c)+\frac{3}{2}O_2(g) \rightarrow KTaO_3$ [-12.04 eV (Ref. 24)] as parts of the Born-Haber cycle. Since the reliability of these values is hard to estimate, the comparison between theory and experiment should not be overestimated in this case.

B. Band structures

The band structures of $KNbO_3$ and $KTaO_3$ have been calculated with the theoretical lattice constants a_{energy} of Table II. The result for $KNbO_3$ is shown in Fig. 1. The

TABLE II. Lattice constant a (Å), bulk modulus B (Mbar), and cohesive energy E_{coh} (eV/unit cell).

ABO_3	a_{energy}	a_{pressure}	$a_{\mathrm{expt.}}$	$B_{\mathrm{calc.}}$	$B_{\mathrm{expt.}}$	$E_{\mathrm{coh}}^{\mathrm{calc.}}$	$E_{\mathrm{coh}}^{\mathrm{expt.}}$
$KNbO_3$	3.94	3.97	$\sim$ 4.0[a]	2.47	$\sim$ 1.38[b]	–42.19	–34.84[c]
$KTaO_3$	3.91	3.94	3.99[d]	2.25	2.30[e]	–44.50	–28.84[c]

[a]Reference 20: extrapolated value for 0 K from lattice constants of the cubic high-temperature phase.
[b]Reference 21: calculated from cubic elastic constants.
[c]A Born-Haber cycle has been performed to get the experimental values. Heats of formation were taken from Refs. 23–25.
[d]Reference 1.
[e]Reference 22: calculated from cubic elastic constants.

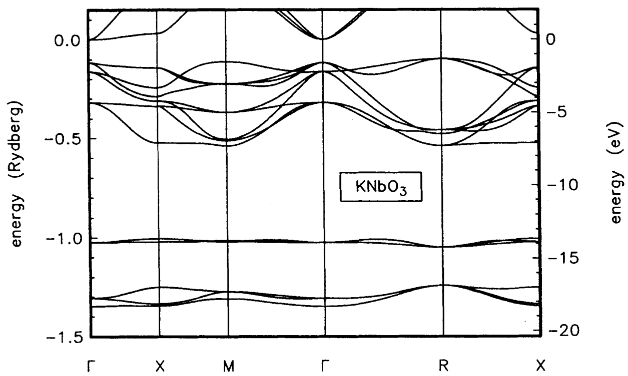

FIG. 1. Calculated band structure of $KNbO_3$.

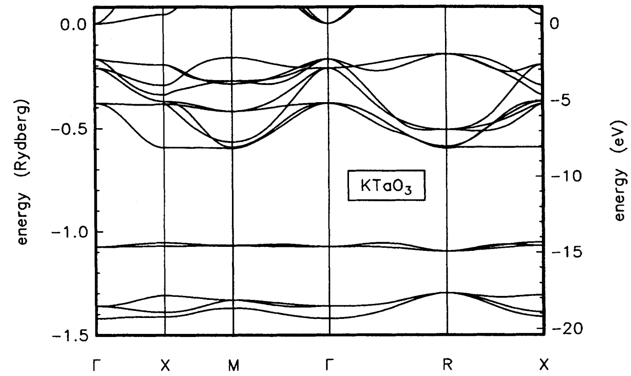

FIG. 2. Calculated band structure of $KTaO_3$.

occupied bands of Fig. 1 mainly consist of three parts: The valence band complex ranging from −2 to −8 eV that is formed by strongly hybridized O(2p)/Nb(4d) states. The bands near −14 eV represent the K(3p) states and those near −18 eV the O(2s) states. The zero of the energy scale in Fig. 1 lies in the conduction-band edge at the Γ point, which is made out of Nb(4d) states.

As expected, the band structure of $KTaO_3$ in Fig. 2 exhibits a strong similarity to that of $KNbO_3$. The valence bands now are formed by O(2p)/Ta(5d) states and the conduction-band edge at Γ (zero energy) is made out of Ta(5d) states. The only significant difference between both band structures lies in the size of the calculated bandgap $E_{\rm gap}$, which for $KTaO_3$ ($E_{\rm gap}$ = 2.1 eV) is 0.7 eV larger compared to $KNbO_3$ ($E_{\rm gap}$ = 1.4 eV). This result agrees qualitatively with the corresponding experimental data 3.79 eV [determined from Faraday rotation at 77 K (Ref. 1)] and ∼ 3.3 eV [extrapolated to 0 K from gap energies (α = 100 cm^{-1}) of the high-temperature cubic phase[21]] for $E_{\rm gap}$, however, the calculation underestimates $E_{\rm gap}$ by about 50%. Too small values for bandgaps are a well-known shortcoming of DFT when combined with the LDA and applied to semiconductors and insulators.[26]

We found that the fundamental bandgaps of $KNbO_3$ and $KTaO_3$ are indirect, since the valence-band maxima of both materials lie at R, while the conduction-band minima are at the center Γ of the Brillouin zone. In the case of $KTaO_3$ this result is confirmed by two photon absorption measurements,[27] whereas the experimental situation for $KNbO_3$ seems not to be clear. It must be mentioned, however, that the calculated difference in the local valence-band maxima at Γ and R is only 0.1 eV, and slight changes in the band scheme could therefore change this situation. The results are in qualitative agreement with the recently performed OLCAO calculation for $KNbO_3$;[6] the energy separation between R and Γ is, however, larger in that investigation. Though the valence bandwidth found in that calculation is about 1 eV smaller than ours, both calculated valence band structures are quite similar.

If we compare our results in Figs. 1 and 2 with the corresponding non-self-consistent calculations in Refs. 7–9 we find serious discrepancies. For $KNbO_3$ (Refs. 8 and 9) the calculated valence bandwidth agrees quite well, but the relative position of the K(3p) state differs drastically from our calculation. The O(2s) position is quite similar to that of our calculation; the dispersion, however, is nearly twice as large. For $KTaO_3$ both valence bandwidth (Ref. 7) and K(3p) states (Ref. 9) are quite far away from the present results. This clearly shows that these early calculations have suffered from two deficiencies, namely, not being self-consistent and not being relativistic.

C. Comparison with PES data

In order to compare the theoretical electronic structure with experimental data, photoelectron spectroscopy (PES) experiments have been performed on $KNbO_3$ and $KTaO_3$ at various photon energies $\hbar\omega$. The experiments have been obtained using synchrotron radiation from the storage ring at Berliner Elektronenspeicherring-Gesellschaft für Synchrotronstrahlung m.b.H. (BESSY). The photoelectron spectra have been recorded with an angle-dispersing electron spectrometer(ADES) 400 spectrometer. The measured spectra are compared with the calculated density of states (DOS), which was obtained by using the linear tetrahedron method[28] with 165 k points in the irreducible part of the Brillouin zone. The DOS was convoluted with a Gaussian of 2.5 eV full width at half maximum and a suitably chosen normalization to take into account the experimental broadening, which is dominated by lifetime effects. They are in the range of more than 2 eV. The resolution of the spectrometer was better than 1 eV, and even a higher one would not have improved the resolution of the spectrum. A correction for the variation of the photoemission cross section with $\hbar\omega$ was not introduced at this stage, so we will mainly concentrate on a comparison of relative energetic positions rather than the shape of the electronic spectra. The results are shown in Figs. 3 and 4. Note that in these figures the zero of the energy scale still coincides with the calculated conduction-band minimum. The reference level has been chosen in such a way that the first measured peak A in the valence spectra roughly fits the theoretical one.

There is good agreement between the experimental

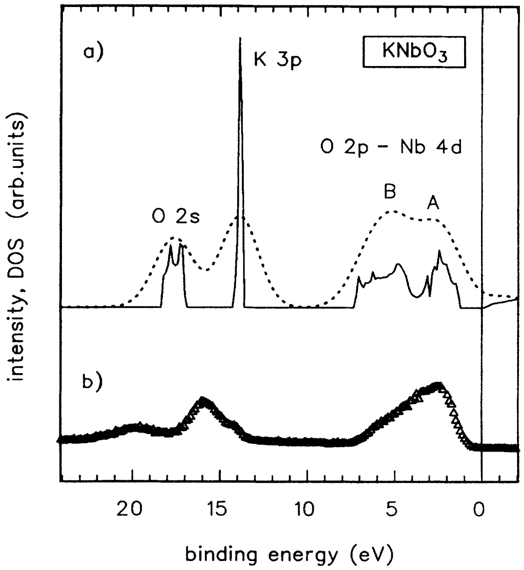

FIG. 3. Comparison of (a) theoretical DOS and (b) experimental x-ray photoelectron spectrum ($\hbar\omega$ = 100 eV) of $KNbO_3$.

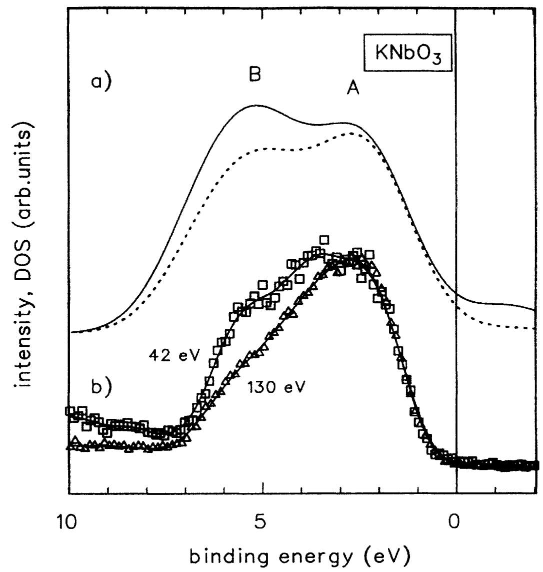

FIG. 5. The influence of d states in the valence-band region of $KNbO_3$: (a) theoretical DOS (solid line: total; dashed line: sp part) and (b) experimental PES.

and the theoretical spectra, although emission from the O($2s$) states is found at about 2 eV higher binding energies when compared with theory (cf. Figs. 3 and 4). The experimental K($3p$) peak appears to be split. The more intense peak at higher binding energy has to be attributed to emission from K atoms at the surface. At kinetic energies of about 130 (100) eV, the escape depth of the photoemitted electrons is very small, leading to a high surface sensitivity. From x-ray photoemission spectra measurements we know that only the shoulder of the K($2p$) peak originates in excitation from bulk electronic states. This energetic position agrees very well with the theoretical value.

For the valence states, calculated and measured bandwidths are nearly equal. The main difference between theory and experiment in Figs. 3 and 4 is the supression of the calculated peak B in the measurements relative to peak A. An explanation for this effect is the l dependence of the photoelectron cross section, which has not been taken into account in the calculation. The measurements in Figs. 3 and 4 have been done for an excitation energy $\hbar\omega$ = 130 (100) eV, which is in between the Cooper minima for excitation of Nb $4d$ (85 eV) and Ta $5d$ (185 eV) atomic states.[29] This choice of $\hbar\omega$ obviously is

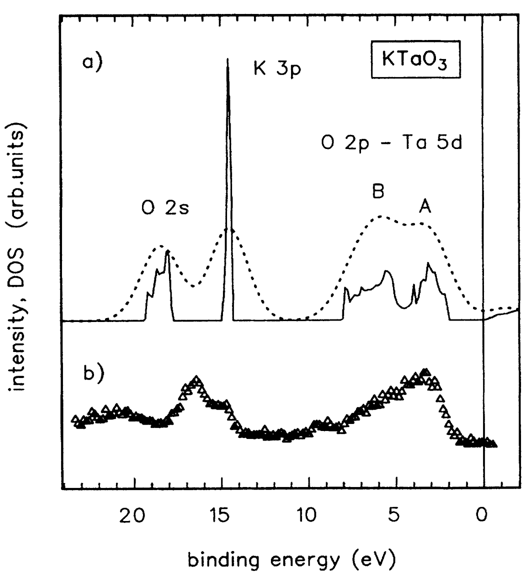

FIG. 4. Comparison of (a) theoretical DOS and (b) experimental x-ray photoelectron spectrum ($\hbar\omega$ = 130 eV) of $KTaO_3$.

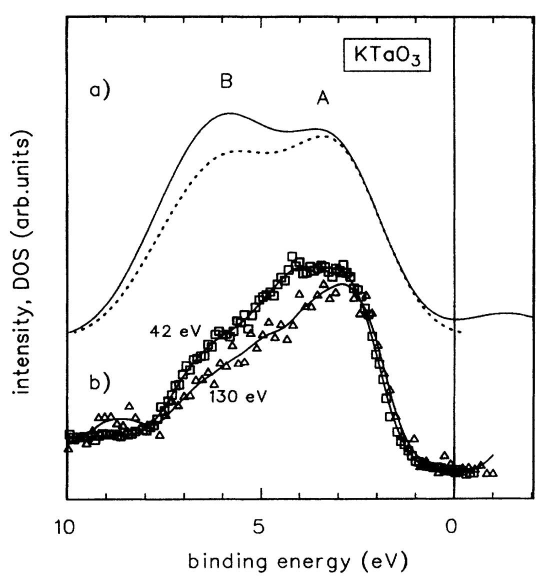

FIG. 6. The influence of d states in the valence-band region of $KTaO_3$: (a) theoretical DOS (solid line: total; dashed line: sp part) and (b) experimental PES.

TABLE III. Number of valence electrons partitioned according to site and angular momentum. [For potassium the p contribution of two different principal quantum numbers (i.e., $3p$ and $4p$) is summed up, leading to $Q_p^{\mathrm{K}} > 6$.]

	Q_s^{K}	Q_p^{K}	Q_d^{K}	Q_s^{B}	Q_p^{B}	Q_d^{B}	$Q_s^{\mathrm{O_3}}$	$Q_p^{\mathrm{O_3}}$	$Q_d^{\mathrm{O_3}}$
$KNbO_3$	0.34	6.55	0.94	0.52	1.04	2.81	5.19	12.53	0.08
$KTaO_3$	0.35	6.56	0.96	0.58	1.04	2.61	5.17	12.65	0.08

responsible for the supression of peak B, as may be seen from the corresponding experimental spectra for $\hbar\omega = 42$ eV in Figs. 5 and 6. Peak B thus should exhibit a high (Nb,Ta) d character, which in turn may also be verified in our calculation by projecting out the sp part of the total DOS (upper curve in Figs. 5 and 6). In contrast the cross section for O $2p$ atomic states is more or less constant in this range of excitation energies compared to Nb (Ta) d states. Peak A and therefore also the top of the valence band thus has mainly p character.

D. Charge distribution

In Sec. III C we showed, that there is a significant hybridization of Nb $4d$ (Ta $5d$) and O $2p$ states in the valence bands of $KNbO_3$ ($KTaO_3$). This means that the bonding in these systems cannot be purely ionic but must exhibit a large covalent part. In the case of $KNbO_3$ a similar conclusion was already derived several decades ago from the observed quadrupole coupling for ^{93}Nb in nuclear resonance experiments.[30]

In Table III we have summarized the self-consistently calculated valence charges within the different atomic spheres. According to the sphere charge distributions, the chemical formula may roughly be written as $K^{-0.83}Nb^{+0.63}O_3^{+0.20}$ and $K^{-0.87}Ta^{+0.77}O_3^{+0.10}$, respectively. Thus we find a significant deviation from the charge distribution of a prototypical ionic crystal, namely, $A^{+1}B^{+5}O_3^{-6}$.

Due to the strong hybridization between the O p states and the Nb (Ta) d states, there is a large amount of valence charge transfer back to Nb (Ta), revealing that the static Nb (Ta) charge is significantly less than $+5$ and the O sphere is more or less neutral, rather than charged by -2. These ASA sphere charge distributions may simplify the physical reality and also depend on the choice of the radii. However, the radii for the A and B metals (K,Nb,Ta) have been chosen to be quite similar to their values in the pure metal phases. So the fact that Nb, as well as Ta, has a charge deficit less than $+1$ instead of $+5$, cannot be caused by an unreasonably large sphere radius in the present calculation. Similar results have been found for Ti in $SrTiO_3$ and $BaTiO_3$ (Refs. 4 and 5) and also for W in $NaWO_3$ (Ref. 17).

The amount of extra valence charge of -0.83 (-0.87) on the K sphere is surprising, too, and in contradiction with the traditional picture for simple metals. Again hybridization effects, and not an oversized sphere radius, can be seen as responsible for this distribution of charge. Like in the case of $NaWO_3$, this may be pictured as originating in the overlap from the NbO_3 (TaO_3) bonding valence electrons into the K atomic sphere, giving rise to a negative K charge.

ACKNOWLEDGMENTS

St. Witzel and M. Neuber are gratefully acknowledged for their experimental support at BESSY. We wish to thank R. Blachnik for the helpful discussions on the topic of experimental cohesive energies. This work was supported in part by the Bundesministerium für Forschung und Technologie (Contract No. 05 427 AAB a). We are grateful to the Deutsche Forschungsgemeinschaft for financial support through Sonderforschungsbereich (SFB) 225.

[1] *Ferroelectrics and Related Substances*, edited by K.-H. Hellwege, Landolt-Börnstein: Numerical Data and Functional Relationships in Science and Technology, Vol. III/16a Oxides (Springer-Verlag, Berlin, 1981).

[2] J. F. Schooley, W. R. Hosler, and M. L. Cohen, Phys. Rev. Lett. **12**, 474 (1964).

[3] K.-H. Weyrich and R. Siems, Z. Phys. **61**, 63 (1985).

[4] K.-H. Weyrich and R. P. Madenach, Ferroelectrics **111**, 9 (1990).

[5] R. E. Cohen and H. Krakauer, Phys. Rev. B **42**, 6416 (1990).

[6] Yong-Nian Xu, W. Y. Ching, and R. H. French, Ferroelectrics **111**, 23 (1990).

[7] L. F. Matheiss, Phys. Rev. B **6**, 4718 (1972).

[8] P. Pertosa, F. M. Michel-Calendini, and G. Metrat, Ferroelectrics **21**, 637 (1978).

[9] P. Pertosa and F. M. Michel-Calendini, Phys. Rev. B **17**, 2011 (1978).

[10] F. M. Michel-Calendini, H. Chermette, and J. Weber, J. Phys. C **13**, 1427 (1980).

[11] E. Krätzig and O. F. Schirmer, in *Photorefractive Centers in Electrooptic Crystals*, Topics in Applied Physics, Vol. 61, edited by P. Günter and J.-P. Huignard (Springer-Verlag, Berlin, 1988).

[12] O. K. Andersen, Phys. Rev. B **12**, 3060 (1975).

[13] P. Hohenberg and W. Kohn, Phys. Rev. **136**, B864 (1964).

[14] W. Kohn and L. J. Sham, Phys. Rev. A **140**, A1133 (1965).

[15] U. von Barth and L. Hedin, J. Phys. C **5**, 1629 (1972).

[16] H. L. Skriver, *The LMTO Method* (Springer-Verlag, Berlin, 1984).

[17] N. E. Christensen and A. R. Mackintosh, Phys. Rev. B **35**, 8246 (1987).

[18]N. N. Greenwood and A. Earnshaw, *Chemistry of the Elements* (Pergamon, Oxford, 1984).
[19]R. M. Nieminen and C. H. Hodges, J. Phys. F **6**, 573 (1976).
[20]G. Shirane, R. Newnham, and R. Pepinsky, Phys. Rev. **96**, 581 (1954).
[21]E. Wiesendanger, Ferroelectrics **6**, 263 (1974).
[22]U. Hiromoto and T. Sakudo, J. Phys. Soc. Jpn. **38**, 183 (1975).
[23]Estimated value: P. Spencer (private communication).
[24]G. Jansone, I. S. Vinogradova, N. Zaleckite, and S. E. Rozentsveig, Neorgan. Stekla Pokrytija Mater. **6**, 137 (1983).
[25]R. C. Weast and M. J. Astle, *CRC-Handbook of Chemistry and Physics* (CRC, Boca Raton, 1982-83), Vol. 63.
[26]R. W. Godby, M. Schlüter, and L. J. Sham, Phys. Rev. B **36**, 6497 (1987).
[27]S. I. Shablaev, A. M. Danishevskii, and V. K. Subashiev, Zh. Eksp. Teor. Fiz. **86**, 2158 (1984) [Sov. Phys. JETP **59**, 1256 (1984)].
[28]G. Lehman and M. Taut, Phys. Status Solidi B **54**, 469 (1972).
[29]J. J. Yeh and I. Lindau, At. Data Nucl. Data Tables **90**, 168 (1985).
[30]R. M. Cotts and W. D. Knight, Phys. Rev. **96**, 1285 (1954).